JOTCS A
Journal of the Turkish Chemical Society
Section: A
Chemistry
TURKISH CHEMICAL SOCIETY

Spectral Outputs of Yb^{3+}/Pr^{3+} Doped Tellurite Glasses for Solid-State Lighting

Murat Erdem[1]*, Anıl Doğan[1]
[1]Physics Department, Faculty of Science and Letters, Marmara University, 34722, Istanbul, Turkey

Abstract: Downconversion processes which include visible and near-infrared luminescence at high energy excitation have been investigated in Yb^{3+}/Pr^{3+} doped TeO_2-ZnO-BaO glasses. The decrease of the DC emission intensities of Pr^{3+} ions with increasing mol% amount of Pr^{3+} ions is attributed to the concentration quenching. The CIE chromaticity coordinates of the perceived emission of Pr^{3+} ions shifted from orange to the red region depending on the increase in the pumping power. Consequently, Yb^{3+}/Pr^{3+} doped TeO_2-ZnO-BaO glasses could be used as functional optical materials for solid-state lighting applications.

Keywords: Downconversion, tellurite glasses, color parameters, lighting.

Submitted: September 09, 2021. **Accepted:** November 19, 2021.

Cite this: Erdem M, Doğan A. Spectral Outputs of Yb3+/Pr3+ Doped Tellurite Glasses for Solid-State Lighting. JOTCSA. 2022;9(1):21–8.

DOI: https://doi.org/10.18596/jotcsa.993096.

***Corresponding author. E-mail:** merdem@marmara.edu.tr.

INTRODUCTION

Downconversion (DC), which is known as Quantum Cutting (QC), is a frequency conversion process that a photon at higher energy is cut into two photons at lower energy. This physical energy conversion process has represented by Dexter in the 1950s (1). Energy conversion processes play an important role in studies on rare earth (RE) ion doped materials for assorted areas, for instance, lighting technology, solar cells, optical amplifiers, and solid-state lasers (2-5). Among the RE ions, Pr^{3+} ions can exhibit multi-photon emission under a high energy excitation, as an instance of downconversion (6). Besides, the luminescence performance of Pr^{3+} ions can be enhanced by contributing the ideal rate of Yb^{3+} ions as an acceptor in the energy transfer (ET) processes between both ions (7). Therefore, Yb^{3+} ion provides a phonon-assisted non-resonant energy transfer. Also, the phonon structure of the material is important due to the achievement of efficient phonon-assisted energy transfer (8).

Tellurite glasses have common usage in optical fibers, mid-infrared laser applications, and optical sensors (9-11) due to having attractive features such as wide transmission frame, high refractive indices, lower melting temperature, high thermal stability against crystallization, good chemical durability, high devitrification resistance, low phonon energy, and high RE ion solubility (12,13).

With modifier oxides (ZnO, BaO, GeO, Nb_2O_5, and B_2O_3, etc), the physical properties of tellurite-based glass materials can change. Among them, ZnO indicates that a decrease in the optical band gap, glass density, and thermal stability, whereas an increment in the refractive index, crystallization temperature (T_c), and glass transition temperature (T_g) (14,15). BaO also provides higher T_g, thermal stability, transmission spectra, and the cross-linking network density to glass materials (16,17). Additionally, high BaO concentrations in the Er^{3+} doped phosphate glasses give rise to intense red and near-infrared (NIR) emissions (18).

The studies on Pr^{3+} and Yb^{3+}/Pr^{3+} doped glass materials are available in the literature. In the

studies on Pr^{3+} doped TeO_2–Sb_2O_3–WO_3 and TeO_2-ZnO-YF_3-$NaYF_4$ glass systems, it is seen that the luminescence intensities of Pr^{3+} doped glasses increase with increasing Pr^{3+} concentration up to 1.0 mol%, and then decrease over the 1.0 mol%. This decrement is proposed to be due to concentration quenching (19,20). The emission of Pr^{3+} ions around 910 nm corresponding to $^3P_0 \rightarrow {}^1G_4$ transition decreases down to zero at 6 mol% Yb^{3+} ion concentration, and $^2F_{5/2} \rightarrow {}^2F_{7/2}$ emission intensity at 978 nm of Yb^{3+} ions decrease by increasing Yb^{3+} ion concentration due to the reabsorption process of Yb^{3+} (21). The range of 1050 nm emission of Pr^{3+} ions which is attributed to $^1D_2 \rightarrow {}^3F_{3,4}$ energy transition as an occurrence by the cross-relaxation process of $^3P_0 + {}^3H_4 \rightarrow {}^3H_6 + {}^1D_2$ in Yb^{3+}/Pr^{3+} co-doped SiO_2-Nb_2O_5 nanocomposites had been reported (22). The energy transition from $^2F_{5/2}$ level to $^2F_{7/2}$ level of Yb^{3+} ion can be observed at around 1020 nm as seen in our results due to the cross-relaxation between Pr^{3+} and Yb^{3+} ions correspond to $^3P_0 + {}^2F_{7/2} \rightarrow {}^1G_4 + {}^2F_{5/2}$ (23). Rajesh et. al. reported that the emission intensity of Yb^{3+}: $^2F_{5/2} \rightarrow {}^2F_{7/2}$ transition decreased with increasing Yb^{3+} ion concentration due to the back energy transfer process from $^2F_{5/2}$ level of Yb^{3+} to $^1G_4$ level of Pr^{3+} ions (24). Marcos P. Belançon et. al. was investigated the 612 and 645 nm emissions of Pr^{3+} doped TWNN glasses at lower and higher Pr^{3+} concentrations and obtained stronger 645 nm and weaker 612 nm emissions at high Pr^{3+} concentration due to hypersensitive $^3P_0 \rightarrow {}^3F_2$ transition of Pr^{3+} ions (25). Seshadri et al. proposed that the Yb^{3+}/Pr^{3+} co-doped TBZLN glasses are good candidates for photonic devices due to their yellow-orange emissions (26). V. Himamaheswara Rao et.al observed the orange color on Pr^{3+} ions doped TeO_2–Sb_2O_3–WO_3 glasses (27). Furthermore, reddish-orange color was observed on the Commission International de L'Eclairage (CIE, France) chromaticity system under 445 nm excitation in Pr^{3+} doped ZnO-Na_2CO_3-Bi_2O_3-B_2O_3 glasses which are applicable materials for lighting devices (28).

Apart from these studies in the literature, in our study, the DC and tunable color properties of Yb^{3+} and Pr^{3+} ion-doped TeO_2-ZnO-BaO (TZB) glasses under 439 nm laser excitation were examined and discussed.

MATERIALS AND METHODS

Yb^{3+}/Pr^{3+} ions doped TZB glasses were produced by melt quenching which is the traditional technique for fabricating the glass materials. The powder's purities of oxides are 99.995% TeO_2 and 99.999% BaO by Sigma Aldrich; 99.999% ZnO, 99.9% Pr_2O_3, and 99.99% Yb_2O_3 by Alfa Aesar. The mol percent values of the oxide powers are (76-x)% for tellurium dioxide, 16% for zinc oxide, 5% for barium oxide, x% for praseodymium oxide, and 3% for ytterbium oxide. The x values of praseodymium oxides are chosen as 0.075 and 0.15 mol and the glass samples are labeled as TZBYP1 and TZBYP2 respectively.

The oxide powders whose amounts were defined and mixed in an agate mortar. The melt of the mixture was obtained in the furnace at 950 °C for 1 h. The molten mixture was poured from a platinum crucible into a stainless-steel mold. To abate the inner stress, the melt was heated at 150 °C in the stainless-steel mold and kept for 30 minutes. After manufacturing, transparent TZBYP glasses were prepared for the optical analyses.

The absorption spectrum of the samples was obtained through A Perkin Elmer Lambda 35 UV/VIS Spectrophotometer at room temperature. The analysis of photoluminescence spectra of the glasses was done via an SP2500i monochromator from Princeton Instruments. To define the emission intensities of the samples, a SI 440-silicon detector from the Acton series was used. A CNI MDL-H-975 model continuous-wave diode laser was used to excite the glass samples. The pump power applied on the glass samples was determined through a FieldMaxII - TOP power meter from Coherent. To specify the chromaticity coordinates of the luminescence of the samples, an AsenseTek Lighting Passport Model illuminance meter was used.

RESULTS AND DISCUSSIONS

Absorption Spectra

Figure 1 illustrates the absorption spectra of TZBYP glasses in the range of 400-1100 nm. In the spectra, four absorption peaks are observed at 435, 445, 485, and 628 nm wavelengths correspond to the ground level ($^3H_4$) excitation to the $^3P_2$, $^3P_1$, 1I6, $^3P_0$ and $^1D_2$ excited energy levels of the Pr^{3+} ions, respectively. Additionally, the broad absorption band of Yb^{3+} ions is observed around 1065 nm due to the $^2F_{7/2} \rightarrow {}^2F_{5/2}$ transitions. Moreover, as seen in the spectra, there is a rise in the absorption band peaks depending on the increasing concentration of Pr^{3+} ions.

Photoluminescence Characteristics

Figure 2 indicates the DC luminescence intensities of two glasses between 400-1100 nm wavelengths. As seen in Figure 2, the peaks of down-converted emissions of Pr^{3+} ions centered around 497, 530, 542, 597, 617, 647, 686, 708, and 732 nm at the visible region, and 886 nm at the NIR region. These peaks correspond to the $^3P_0 \rightarrow {}^3H_4$, $^3P_1 \rightarrow {}^3H_5$, $^3P_0 \rightarrow {}^3H_5$, $^1D_2 \rightarrow {}^3H_4$, $^3P_0 \rightarrow {}^3H_6$, $^3P_0 \rightarrow {}^3F_2$, $^3P_1 \rightarrow {}^3F_3$, $^3P_1 \rightarrow {}^3F_4$, $^3P_0 \rightarrow {}^3F_4$ transitions at the visible region and $^1D_2 \rightarrow {}^3F_2$ transition at the NIR region, respectively. Also, the emission observed around

the 1020 nm is due to Yb^{3+}: $^2F_{5/2} \rightarrow {}^2F_{7/2}$ transitions. The spectral output of the glasses indicates that the down-conversion emission intensities decreased with increasing mol% of Pr^{3+} ions on account of the concentration quenching.

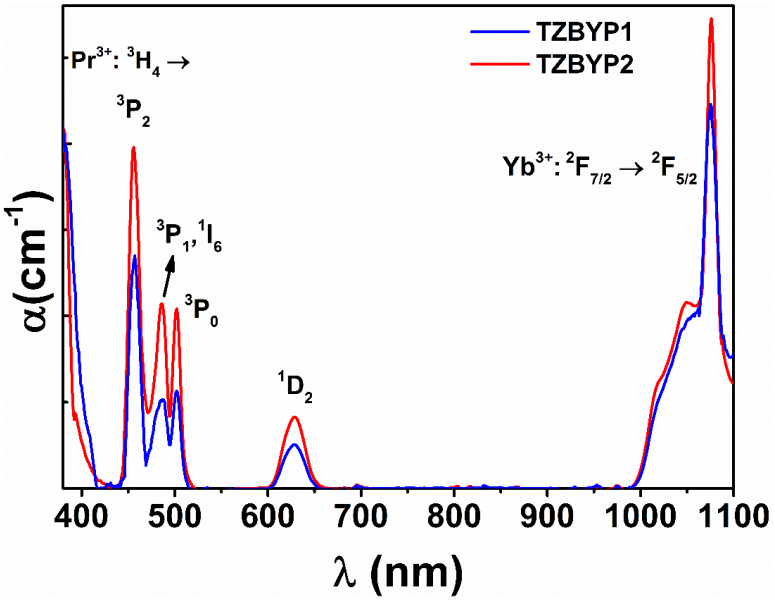

Figure 1: Absorption spectra of TZBYP glasses in 400-1100 nm range.

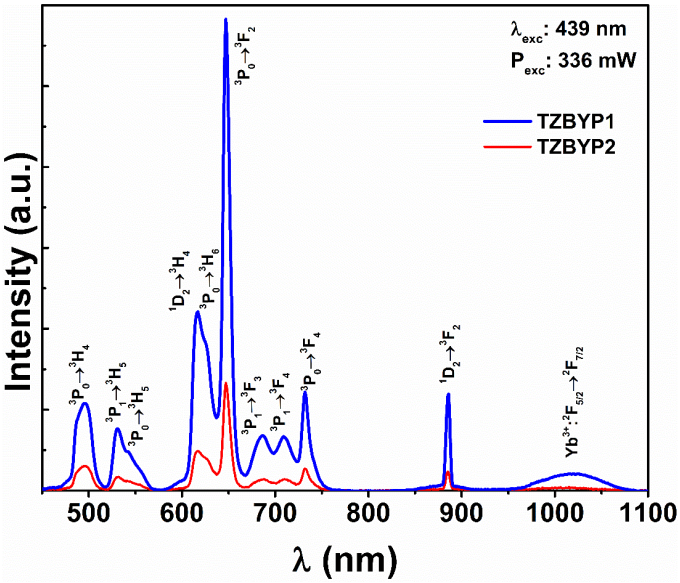

Figure 2: Down-conversion emission intensities depending on the Pr^{3+} concentration.

The DC luminescence intensities of the TZBYP glasses were investigated as the function of the pumping power to explain the DC energy transfer process. Figures 3 and 4 (a) represent the DC emission behaviors of the TZBYP1 and TZBYP2 glasses at various pump powers. As clearly seen in Figures 3 and 4 (a), the emission intensities of both glasses increased with an increasing 439 nm laser pumping power. The plots of the emission intensities versus the pumping powers in the logarithmic scale are demonstrated in Figures 3 and 4 (b) to express the photonic absorption process. The number of photons (n) was calculated by the slope of the luminescence intensity vs. power curve ($I \sim Pn$). The slope values of TZBYP1 glass are found to be n_{497} = 0.84, n_{530} = 0.96, n_{617} = 1.04, n_{647} =1.05, n_{686} = 0.89, n_{708} = 0.82, n_{732} = 0.95, n_{882} = 0.63 and n_{1020} = 0.52, respectively. For TZBYP2 glass, the values are n_{497} = 0.91, n_{530} = 1.05, n_{617} = 1.03, n_{647} = 1.03, n_{686} = 0.98, n_{708} = 0.94, n_{732} = 0.96, n_{882} = 0.3 and n_{1020} = 0.55, respectively. These results indicate that the down-conversion energy process is due to one-photon absorption.

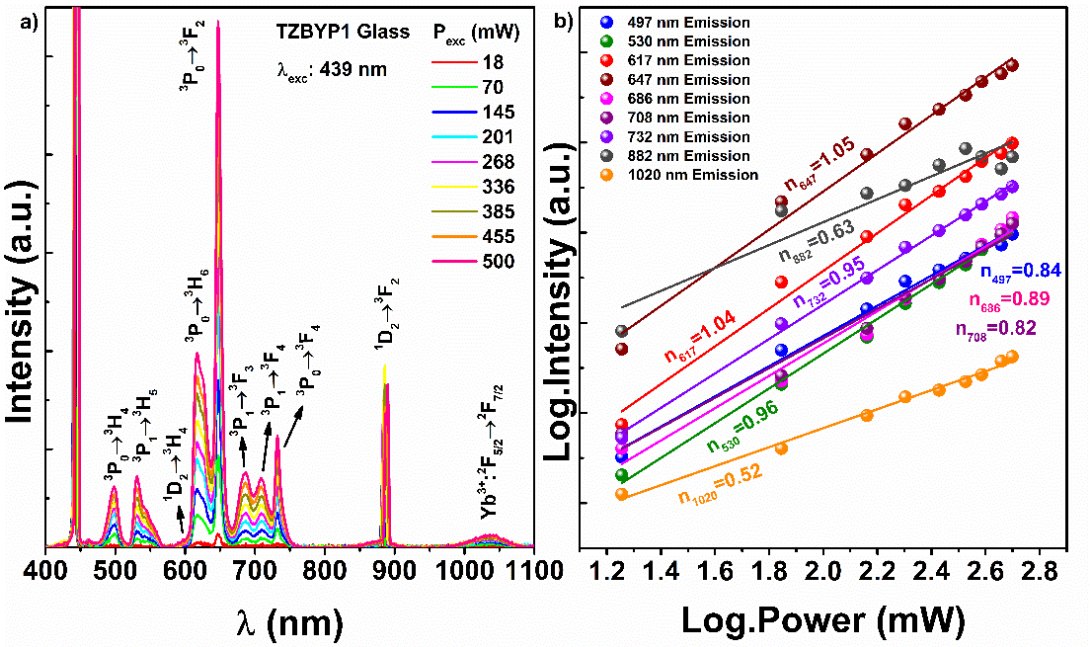

Figure 3: (a) Down-conversion luminescence at different pump powers, and (b) the intensity-power curves for the emissions of TZBYP1.

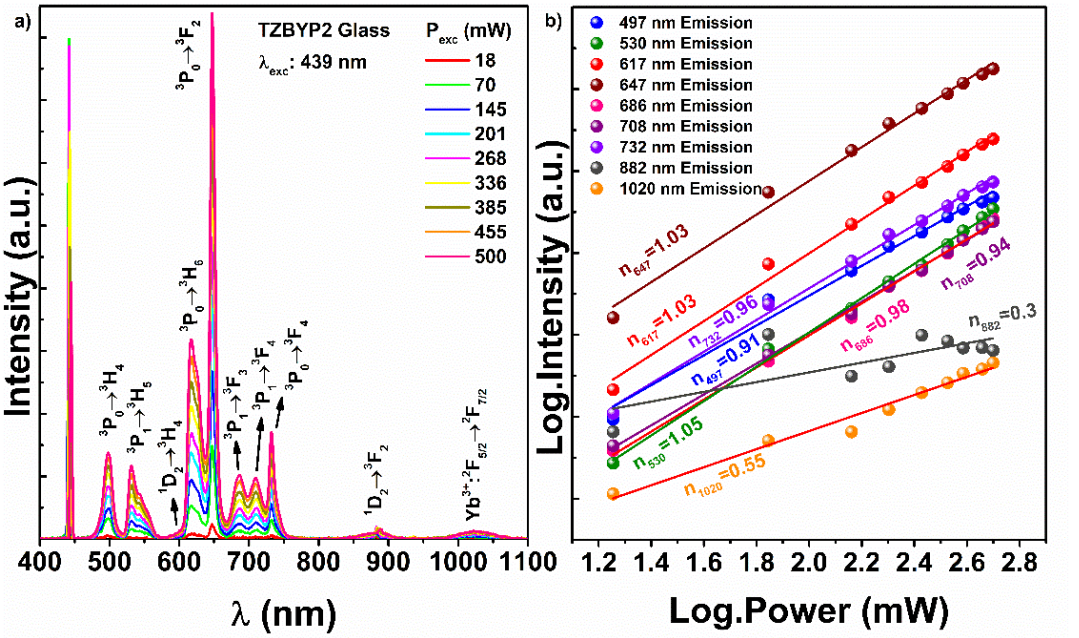

Figure 4: (a) Down-conversion luminescence at different pump powers, and (b) the intensity-power curves for the emissions of TZBYP2.

Energy Transfer Mechanism

The schematic representation of the energy levels of Yb^{3+} and Pr^{3+} ions at visible and NIR regions is given and the possible energy transfers (ET1 and ET2) in the DC process in the Yb^{3+}/Pr^{3+} doped tellurite glasses are defined in Figure 5. At first, Pr^{3+} ions are excited by 439 nm blue photon from the multiplet $^3H_4$ ground state to the multiplet ^3P_j excited state. Nonradiative relaxations (NR) take place from $^3P_2$ state to $^3P_0$ state that is mostly populated and from $^3P_0$ state to $^1D_2$ state. The possible energy transfers between the Pr^{3+} and Yb^{3+} ions are given by the two-step sequential resonant energy transfer (29) from $^3P_0$ $^1G_4$ transition of Pr^{3+} ions to $^2F_{7/2} \rightarrow {}^2F_{5/2}$ transition of Yb^{3+} ions and followed by from $^1G_4 \rightarrow {}^3H_4$ transition of Pr^{3+} ions to $^2F_{7/2} \rightarrow {}^2F_{5/2}$ transition of Yb^{3+} ions. The energy difference between $^3P_0$ and $^1G_4$ levels of Pr^{3+} ions is close to the energy difference between $^2F_{7/2}$ and $^2F_{5/2}$ levels of Yb^{3+} ions. Moreover, the energy gap between the lowest Stark and sub-Stark energy levels of $^2F_{5/2}$ levels of Yb^{3+} ion is

small. Therefore, the energy transition from Pr^{3+} ion to Yb^{3+} ion loads the sub-Stark level of $^2F_{5/2}$ state of Yb^{3+} ion and the energy transfer from the minimum Stark level of $^2F_{5/2}$ state to the minimum Stark and sub-Stark levels of $^2F_{7/2}$ state causes the emission at 1040 nm (30).

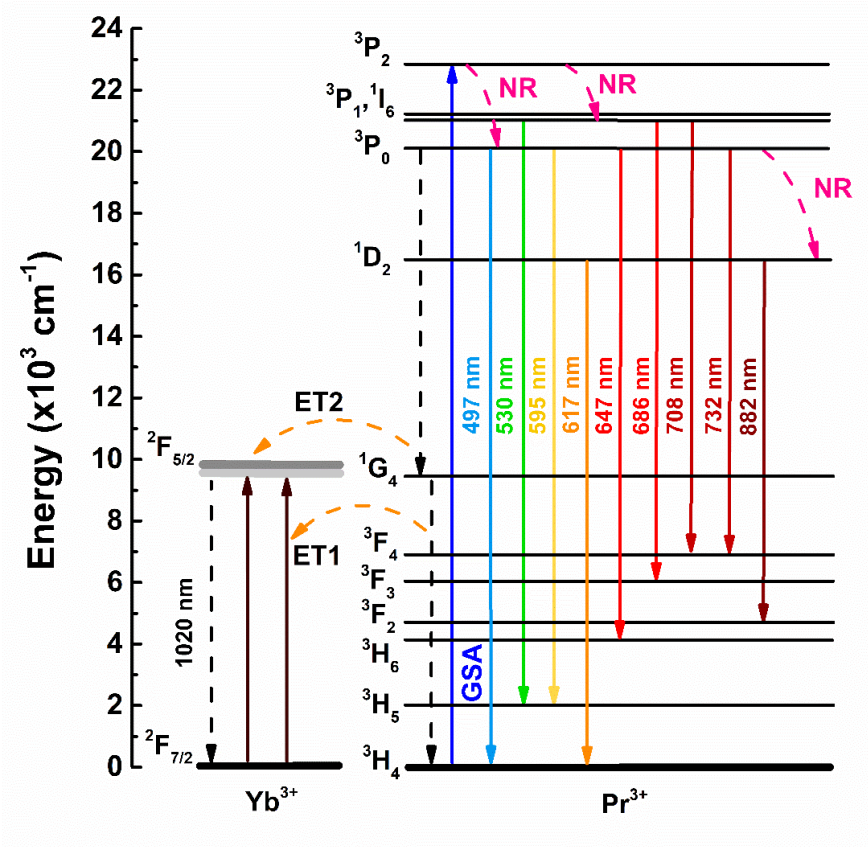

Figure 5: Energy level diagram of Pr^{3+} and Yb^{3+} ions in the TZB glasses.

Color Analysis

Figures 6 and 7 show the photometric analysis supplied from the illuminance meter for the glasses. The insets in Figures 6 and 7 also indicate the camera image of the TZBYP glasses. As seen in the CIE chromaticity diagram of the TZBYP glasses, the color coordinates change with the laser pumping power. While the color coordinate values of TZBYP1 glass were measured as (0.57; 0.42), (0.64; 0.33), (0.63; 0.34) and (0.67; 0.32) for the related pump power of 70, 201, 336 and 455 mW, respectively. These values of the color coordinates were measured as (0.56; 0.38), (0.54; 0.43) and (0.69; 0.31) for TZBYP2 glass at the pumping power of 201, 336 and 385 mW, respectively. As seen in both figures, remarkable shifts observed in the coordinates with increasing pump power are from the orange to the red region in the CIE diagram.

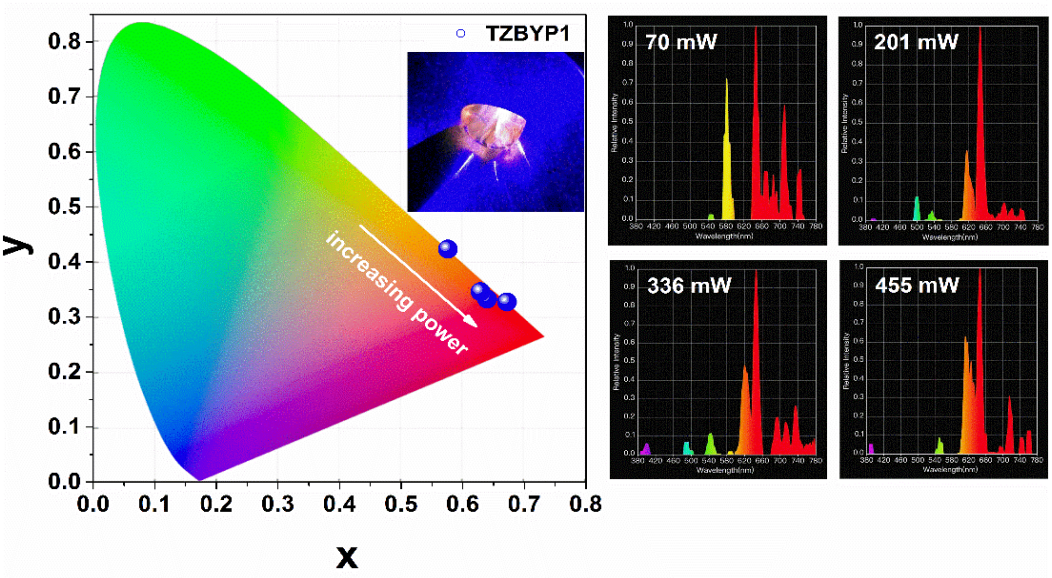

Figure 6: Color coordinates in the CIE diagram and luminescence spectra of TZBYP1 glass at different pumping powers.

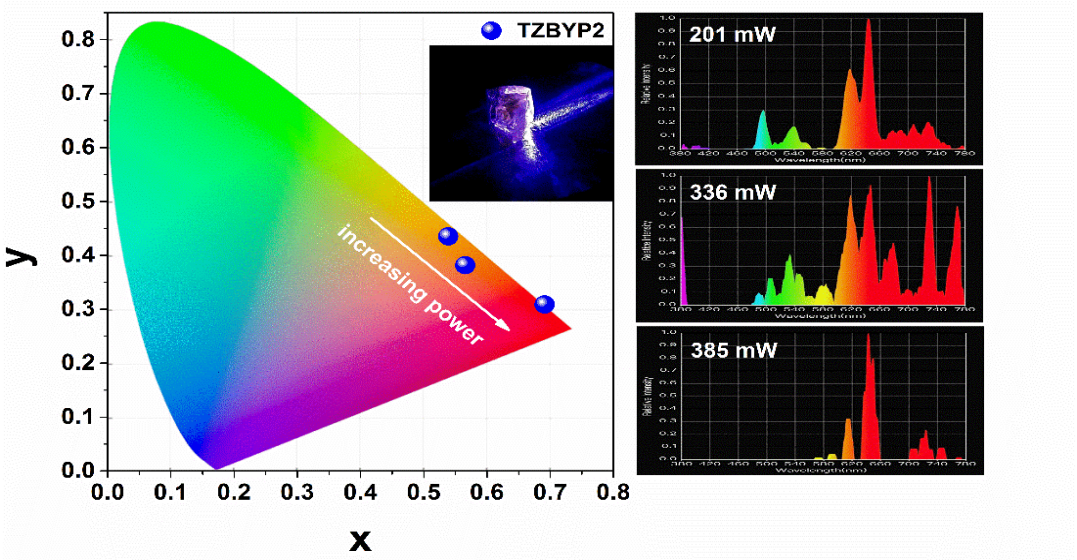

Figure 7: Color coordinates in the CIE diagram and luminescence spectra of TZBYP2 glass at different pumping power.

CONCLUSION

TeO_2-ZnO-BaO glasses doped with Yb^{3+} and Pr^{3+} ions were produced by the traditional melt quenching method. Intense multi-photon downconversion luminescence in the visible region was observed under a 439 nm laser excitation. The spectral output of the glasses indicated that the increment in the Pr^{3+} concentration quenches the luminescence intensity of Pr^{3+} ions. The color coordinates shifted from the orange region to the red region with increasing excitation power. Consequently, the Yb^{3+}/Pr^{3+} doped TeO_2-ZnO-BaO glasses can be useful material for solid-state lighting.

ACKNOWLEDGMENTS

The Scientific Research Projects Unit (BAPKO) of Marmara University financially supported this study with the FEN-C-YLP-141118-0600 grant number.

REFERENCES

1. Dexter DL. Possibility of Luminescent Quantum Yields Greater than Unity. Phys Rev. 1957 Nov 1;108(3):630–3. <URL>.

2. Caldiño U, Bettinelli M, Ferrari M, Pasquini E, Pelli S, Speghini A, et al. Rare Earth Doped Glasses

for Displays and Light Generation. In 2014 [cited 2021 Nov 21]. p. 174–8. Available from: <URL>.

3. Belançon MP, Marconi JD, Ando MF, Barbosa LC. Near-IR emission in Pr3+single doped and tunable near-IR emission in Pr3+/Yb3+ codoped tellurite tungstate glasses for broadband optical amplifiers. Optical Materials. 2014 Apr;36(6):1020–6. <DOI>.

4. Lakshminarayana G, Qiu J. Near-infrared quantum cutting in RE3+/Yb3+ (RE=Pr, Tb, and Tm): GeO2–B2O3–ZnO–LaF3 glasses via downconversion. Journal of Alloys and Compounds. 2009 Jul;481(1–2):582–9. <DOI>.

5. Pask HM, Tropper AC, Hanna DC. A Pr3+-doped ZBLAN fibre upconversion laser pumped by an Yb3+-doped silica fibre laser. Optics Communications. 1997 Jan;134(1–6):139–44. <DOI>.

6. Zhou X, Deng Y, Jiang S, Xiang G, Li L, Tang X, et al. Investigation of energy transfer in Pr3+, Yb3+ co-doped phosphate phosphor: The role of 3P0 and 1D2. Journal of Luminescence. 2019 May;209:45–51. <DOI>.

7. Borrero-González LJ, Nunes LAO, Carmo JL, Astrath FBG, Baesso ML. Spectroscopic studies and downconversion luminescence in OH−-free Pr3+–Yb3+ co-doped low-silica calcium aluminosilicate glasses. Journal of Luminescence. 2014 Jan;145:615–9. <DOI>.

8. Bose S, Debnath R. Strong crystal-field effect and efficient phonon assisted Yb3+→Tm3+ energy transfer in a (Yb3+/Tm3+) co-doped high barium–tellurite glass. Journal of Luminescence. 2014 Nov;155:210–7. <DOI>.

9. Lousteau J, Boetti N, Chiasera A, Ferrari M, Abrate S, Scarciglia G, et al. Er(3+) and Ce(3+) Codoped Tellurite Optical Fiber for Lasers and Amplifiers in the Near-Infrared Wavelength Region: Fabrication, Optical Characterization, and Prospects. IEEE Photonics J. 2012 Feb;4(1):194–204. <DOI>.

10. Wang R, Meng X, Yin F, Feng Y, Qin G, Qin W. Heavily erbium-doped low-hydroxyl fluorotellurite glasses for 27 μm laser applications. Opt Mater Express. 2013 Aug 1;3(8):1127. <DOI>.

11. Leal JJ, Narro-García R, Flores-De los Ríos JP, Gutierrez-Mendez N, Ramos-Sánchez VH, González-Castillo JR, et al. Effect of TiO2 on the thermal and optical properties of Er3+/Yb3+ co-doped tellurite glasses for optical sensor. Journal of Luminescence. 2019 Apr;208:342–9. <DOI>.

12. Leal JJ, Narro-García R, Desirena H, Marconi JD, Rodríguez E, Linganna K, et al. Spectroscopic properties of tellurite glasses co-doped with Er3+ and Yb3+. Journal of Luminescence. 2015 Jun;162:72–80. <DOI>.

13. Wang JS, Vogel EM, Snitzer E. Tellurite glass: a new candidate for fiber devices. Optical Materials. 1994 Aug;3(3):187–203. <DOI>.

14. Elkhoshkhany N, Essam O, Embaby AM. Optical, thermal and antibacterial properties of tellurite glass system doped with ZnO. Materials Chemistry and Physics. 2018 Aug;214:489–98. <DOI>.

15. Ramamoorthy RK, Bhatnagar AK. Effect of ZnO and PbO/ZnO on structural and thermal properties of tellurite glasses. Journal of Alloys and Compounds. 2015 Feb;623:49–54. <DOI>.

16. Manikandan N, Ryasnyanskiy A, Toulouse J. Thermal and optical properties of TeO2–ZnO–BaO glasses. Journal of Non-Crystalline Solids. 2012 Mar;358(5):947–51. <DOI>.

17. Burtan-Gwizdala B, Reben M, Cisowski J, Szpil S, Yousef ES, Lisiecki R, et al. Thermal and spectroscopic properties of Er3+-doped fluorotellurite glasses modified with TiO2 and BaO. Optical Materials. 2020 Sep;107:109968. <DOI>.

18. Kuwik M, Pisarska J, Pisarski WA. Influence of Oxide Glass Modifiers on the Structural and Spectroscopic Properties of Phosphate Glasses for Visible and Near-Infrared Photonic Applications. Materials. 2020 Oct 23;13(21):4746. <DOI>.

19. Rao VH, Prasad PS, Babu KS. Visible luminescence characteristics of Pr3+ ions in TeO2–Sb2O3–WO3 glasses. Optical Materials. 2020 Mar;101:109740. <DOI>.

20. Rajesh D. Pr3+ doped new TZYN glasses and glass-ceramics containing NaYF4 nanocrystals: Luminescence analysis for visible and NIR applications. Optical Materials. 2018 Dec;86:178–84. <DOI>.

21. Maalej O, Boulard B, Dieudonné B, Ferrari M, Dammak M, Dammak M. Downconversion in Pr3+–Yb3+ co-doped ZBLA fluoride glasses. Journal of Luminescence. 2015 May;161:198–201. <DOI>.

22. Muscelli WC, Aquino FT, Caixeta FJ, Nunes LRR, Zur L, Ferrari M, et al. Yb3+ concentration influences UV–Vis to NIR energy conversion in nanostructured Pr3+ and Yb3+ co-doped SiO2-Nb2O5 materials for photonics. Journal of Luminescence. 2018 Jul;199:454–60. <DOI>.

23. Lakshminarayana G, Qiu J. Near-infrared quantum cutting in RE3+/Yb3+ (RE=Pr, Tb, and Tm): GeO2–B2O3–ZnO–LaF3 glasses via downconversion. Journal of Alloys and Compounds. 2009 Jul;481(1–2):582–9. <DOI>.

24. Rajesh D, Dousti MR, Amjad RJ, de Camargo ASS. Quantum cutting and up-conversion investigations in Pr 3+ /Yb 3+ co-doped oxyfluoro-tellurite glasses. Journal of Non-Crystalline Solids. 2016 Oct;450:149–55. <DOI>.

25. Belançon MP, Marconi JD, Ando MF, Barbosa LC. Near-IR emission in Pr3+single doped and tunable near-IR emission in Pr3+/Yb3+ codoped tellurite tungstate glasses for broadband optical amplifiers. Optical Materials. 2014 Apr;36(6):1020–6. <DOI>.

26. Seshadri M, Bell MJV, Anjos V, Messaddeq Y. Spectroscopic investigations on Yb3+ doped and Pr3+/Yb3+ codoped tellurite glasses for photonic applications. Journal of Rare Earths. 2021 Jan;39(1):33–42. <DOI>.

27. Rao VH, Prasad PS, Babu KS. Visible luminescence characteristics of Pr3+ ions in TeO2–Sb2O3–WO3 glasses. Optical Materials. 2020 Mar;101:109740. <DOI>.

28. Hegde V, Viswanath CSD, Chauhan N, Mahato KK, Kamath SD. Photoluminescence and thermally stimulated luminescence properties of Pr3+-doped zinc sodium bismuth borate glasses. Optical Materials. 2018 Oct;84:268–77. <DOI>.

29. Zhou X, Wang G, Zhou K, Li Q. Near-infrared quantum cutting in Pr3+/Yb3+ co-doped transparent tellurate glass via two step energy transfer. Optical Materials. 2013 Jan;35(3):600–3. <DOI>.

30. Liang L, Mo Z, Ju B, Xia C, Hou Z, Zhou G. Visible and Near-Infrared emission properties of Yb3+/Pr3+ co-doped lanthanum aluminum silicate glass. Journal of Non-Crystalline Solids. 2021 Apr;557:120578. <DOI>.